Jurnal Teknologi

Full Paper

INVESTIGATING THE EFFECT OF TAPER LENGTH ON SENSITIVITY OF THE TAPERED-FIBER BASED TEMPERATURE SENSOR

Baktiar Musa[a,b*], Yasmin Mustapha Kamil[a], Muhammad Hafiz Abu Bakar[a], Ahmad Shukri Mohd Noor[a], Alyani Ismail[a], Mohd Adzir Mahdi[a,c]

[a]Wireless and Photonic Networks Research Center, Faculty of Engineering, Universiti Putra Malaysia, 43400 UPM Serdang, Selangor, Malaysia
[b]Faculty of Electrical Engineering, Universiti Teknologi MARA Terengganu, 23000 Dungun, Terengganu, Malaysia
[c]Institute of Advanced Technology, Universiti Putra Malaysia, 43400 UPM Serdang, Selangor, Malaysia

Article history
Received
15 August 2015
Received in revised form
15 November 2015
Accepted
30 December 2015

*Corresponding author
baktiar@tganu.uitm.edu.my

Graphical abstract

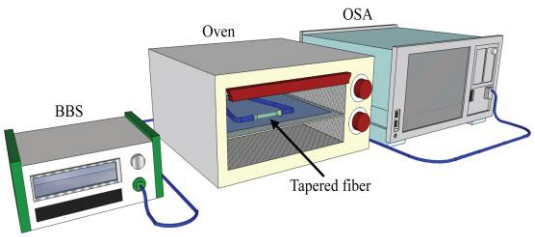

Abstract

A temperature sensor using single-mode tapered fiber is presented. To better understand the behaviour of a tapered optical fiber, transmission experiments with different taper profiles, specifically waist length were performed. The effects of taper profiles on the sensitivity of the sensor were also investigated. It is demonstrated that careful selection of the taper profile can increase the sensitivity of the sensor. In our experiment, a good temperature sensing result was achieved using the optimum parameter. The best sensitivity achieved was 45.5 pm/°C that measured the range of temperature from 30°C to 120°C. The fabricated sensors are easy to fabricate and relatively low cost. Our results indicate that the tapered fiber based temperature sensor has high sensitivity and good repeatability.

Keywords: Fiber optic sensor, tapered fiber, temperature sensor

Abstrak

Suatu sensor suhu menggunakan gentian mod tunggal tirus dibentangkan. Untuk lebih memahami tingkah laku gentian optik tirus, eksperimen penghantaran dengan profil tirus yang berbeza, khususnya panjang pinggang telah dijalankan. Kesan profil tirus ke atas sensitiviti sensor juga disiasat. Ia menunjukkan bahawa pemilihan yang teliti profil tirus boleh meningkatkan sensitiviti sensor. Dalam eksperimen kita, hasilnya suhu penderiaan yang baik telah dicapai menggunakan parameter yang optimum.

Kata kunci: Sensor gentian optik, serat tirus, sensor suhu

1.0 INTRODUCTION

Fiber-optic sensors have attracted a lot of attention due to their excellent properties compared to the traditional electrical-based sensors. Their immunity to electromagnetic interference, small size, easy to integrate with other devices and simplicity in fabrication made them a preferred choice in sensor fabrication [1]. To date, various types and designs of fiber-optic based sensors have been proposed and demonstrated [2]–[4]. Most of the sensors are fabricated using fiber Bragg gratings (FBGs) [5], long-period gratings (LPGs) [6], Mach-Zehnder interferometer [7] and micro-structure fibers such as photonic crystal fibers [8].

Tapered fibers-based sensors have emerged as a notable replacement over other fiber optic-based sensors due to their low cost, easy fabrication and compact structure. Temperature, displacement, and refractive index are the common parameters that can be effectively measured by tapered fiber sensors [9]–[11]. In recent years, the application of tapered fibers is also extended to biosensors [12], [13] and sensors based on surface plasmon resonance [14].

Tapering of an optical fiber results in an increased evanescent field thus enhances the interaction of light with the surrounding medium. Consequently, it is expected that the sensitivity of the sensor will be greatly increase. Temperature monitoring requires a reliable and highly sensitive sensor to record accurate readings over a large temperature gradient especially in harsh environments. In recent years, a number of studies have been dedicated to develop an optical fiber based temperature sensor. For example, temperature sensor based fiber Bragg gratings (FBGs) has been proposed [15]. Another study proposed a fiber fiber-optic Mach–Zehnder interferometeric (MZI) sensor for highly-sensitive and high temperature measurement with a sensitivity of 85.8 pm/°C in the temperature range of 100-400°C [16]. Though most of these sensors have good performance, they require complex fabrication methods and are also relatively expensive. Thus, better alternative temperature sensors that offer simpler fabrication method at a relatively lower cost are greatly needed.

In this work, we propose a tapered fiber-based temperature sensor which is easy to fabricate. Furthermore, it does not require complex grating carving and optical fiber etching technologies. Other advantages of the proposed sensor are compact size, high sensitivity and easy interrogation. These properties offer great prospects of developing practical high temperature sensors for extremely small space and large temperature gradient in harsh environments.

The proposed sensor is fabricated by using a biconical tapered fiber with waist diameter of 10 µm. We are interested to investigate the response of the sensor with the changing temperature. The temperature response of the sensor is indicated by its sensitivity. It is predicted that the taper profile such as taper length, taper angle and waist diameter have significant effects on the sensitivity of the device. Therefore, we believe that by choosing the optimum taper length, the sensitivity of the sensor can be improved. In our proposed sensor, it is demonstrated that the sensitivity is influenced by the taper length. The temperature range in this study is between room temperature to 120°C.

2.0 EXPERIMENTAL

In this study, tapers are fabricated from a single-mode fiber with a core diameter of 8 µm and an overall diameter of 125 µm. After stripping off the outer jacket, the fiber was cleaned with isopropanol alcohol and then placed on the fiber holding blocks (FHBs) of a fiber processing platform (Vytran GPX-3400) for tapering. The Vytran GPX-3400 machine is a highly precise, computer-controlled glass processing machine that utilizes filament as a heat source. The FHBs pulled the fiber to create taper according to the selected profile. The advantages of using this kind of machine compared to the traditional heat-and-pull rig are the uniformity of the waist region. The machine also offers high reproducibility of the taper and the convenience of changing the profile of the tapered fibers. To ensure the uniformity of the taper fabricated in this experiment, the pulling speed of the FHBs was kept at a constant rate of 1 mm/s while the heat transfer rate was set at 38 W.

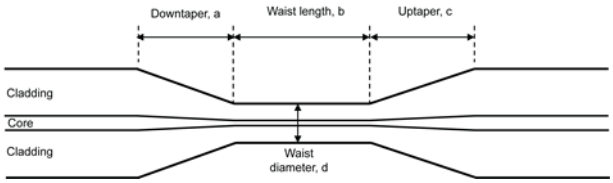

Figure 1 A schematic diagram of a non-adiabatic tapered fiber

Figure 1 shows a schematic diagram of a non-adiabatic tapered fiber which is used as the sensor. The downtaper and uptaper regions, *a* and *c*, are the transition regions where the coupling and recombination of modes occur. The waist diameter, *d* is uniform along the tapered fiber region. In this experiment, the taper length was varied by increasing the waist length, *b* from 4 mm to 12 mm. Note that the overall length of the taper includes the uptaper and downtaper lengths.

To investigate the temperature response with varying taper profile, we fabricated four tapered fibers with different waist lengths. The uptaper and downtaper regions were kept constant at 4 mm so that any changes in the transmission spectrum can be attributed only to the change of waist length. The waist diameter was also fixed at 10 µm. The fabricated sensor was then placed in an oven which

had a temperature range between room temperature and 250°C. After the oven reached the desired temperature, we waited for about 30 minutes for the temperature to stabilize before launching a probe light from an Amonics C+L broadband source (BBS). The transmitted probe light was then detected at the other end by an optical spectrum analyzer (OSA). A transmission spectrum was recorded for every 5°C increase from room temperature to 120°C. Figure 2 illustrates the experimental setup of the fabricated temperature sensor

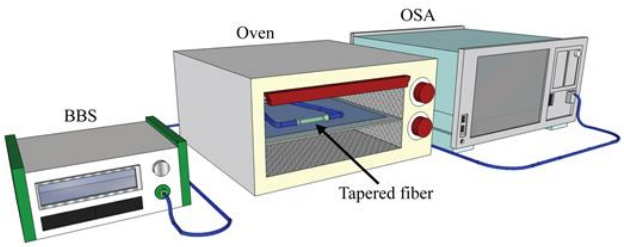

Figure 2 Schematic illustration of the experimental set-up

3.0 RESULTS AND DISCUSSION

Tapering a single-mode fiber involves reducing its diameter by heating a section of the fiber while pulling both its ends, thus creating a biconical transition regions and a relatively long waist region. The waist diameter can be made to be only a few microns over a length of a few centimeters. Under these conditions, the original fiber core becomes so small that it has no significant influence any more, and the light is guided only by the air-glass interface. This enables the light propagating inside the core to penetrate the cladding and subsequently create an evanescent field.

Tapered fibers can be categorized as adiabatic and non-adiabatic depending on the taper angle. If the angle is small enough which enables smooth transition of the optical power, it is categorized as adiabatic taper. In contrast, an abrupt transition due to the large taper angle will produce a non-adiabatic taper. Within non-adiabatic conditions, the taper normally supports more than one mode due to the large difference of the refractive indexes of air and glass. The interference between modes results in the oscillations in the output spectrum. The change of the ambient temperature can significantly change the effective propagation constant of the cladding modes. Thus, tapered fiber can be used as a temperature sensor by monitoring the phase shift of interference fringe.

The transmission spectrum of the tapered fiber is governed by the following equation [17],

$$I_T = I_{co} + I_{cl} + 2\sqrt{I_{co} I_{cl}} \cos\varphi, \quad (1)$$

where I_T is the intensity of the transmission output, I_{co} and I_{cl} are the intensities of the core and cladding modes, respectively. According to Eq. (1), the transmission profile exhibits a series of periodic maxima and minima. Figure 3. shows the spectral response of a tapered fiber with waist length of 4 mm. The transition lengths for both ends are kept at 4 mm each. As predicted, the spectrum of the tapered fiber followed the pattern described by Eq. (1) and it can be seen clearly from the figure that tapering causes the oscillatory behavior of the spectrum. As a reference, the secondary vertical axis displayed the relative transmission spectrum of the tapered fiber. The relative transmission spectrum is defined as the spectrum of tapered fiber subtracted from that of the untapered fiber.

The interference fringe displayed in the spectrum can be explained using the theory of the modal interferometer. When the fundamental mode LP_{01} of the core passed through the down-taper region, it is coupled into the cladding modes LP_{0m} (m is positive integer) thus making a taper to behave like a multimode fiber [15]. However, in the waist region, higher-order LP_{0m} mode suffered greater loss, whereas the lower-order LP_{0m} suffered lower loss during propagation. Consequently, as they enter the up-taper region, the modes recombine into the core mode and the interference between LP_{01} and lower-order LP_{0m} became more dominant. As a result of the coupling and recombination process, the transmission of the taper as a function of the wavelength is oscillatory [18]. Based on the sinusoidal pattern obtained from the tested tapered fiber, it is clear that the interference occurred primarily between the fundamental core mode and only one cladding mode. Higher order modes are filtered out in the waist region because of sharp decrease in the core-cladding diameters. The interference between modes was also reported in a previous study on the properties of tapered fiber [19].

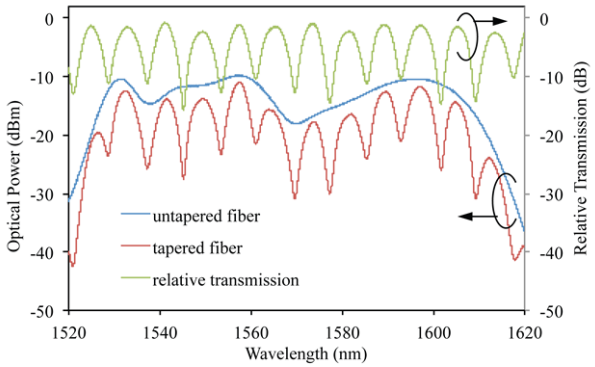

Figure 3 Transmision spectra of the untapered and tapered fibers. Relative transmission of the tapered fiber shows a sinusoidal pattern which indicates the coupling are primarily occurred between the fundamental and the next higher order modes propagating in the tapered fiber

The accumulated phase difference between the two interfering modes is given by the following equation [20]:

$$\varphi = (2\pi\Delta n_{eff}L)/\lambda, \quad (2)$$

where L is the length of tapered fiber, λ is the wavelength of the optical source and the effective index difference, $\Delta n_{eff} = n_{co} - n_{cl}$. The distance between two adjacent peaks/valleys in the spectrum pattern, also known as the free spectral range (FSR), is approximately dependent on the waist length, L as [20]:

$$FSR \approx \frac{\lambda^2}{\Delta n_{eff}L}. \quad (3)$$

It is worth noting that temperature has a distinct effect on refractive index (RI), thermal expansion and thermo-optic properties of the optical fiber. As such, Eq.2 needs to be rewritten as

$$\varphi = \left[2\pi\Delta n_{eff}(T)L(T)\right]/\lambda, \quad (4)$$

where $\Delta n_{eff}(T)$ and $L(T)$ represent the different RI and waist length at temperature T, respectively. Both variables are further defined in Eq. 4(a) and 4(b) [21]

$$L(T) \approx L(T_0)(1+\alpha\Delta T), \quad (4a)$$

$$\Delta n_{eff}(T) \approx \Delta n(T_0)\left[1+\xi\big|_{T=T_0}.\Delta T\right], \quad (4b)$$

where $L(T_0)$ is the waist length at room temperature T_0, α is the thermal expansion coefficient of the fiber material, which in the case of silica is 5.5 x 10^{-7}/°C [22], $\Delta n(T_0)$ is Δn at room temperature (T_0), and ξ is the thermo-optic coefficient. These two equations suggest that when ambient temperature changes, the length of the fiber will change accordingly. This results in the shift of the the interference spectrum, $\Delta\lambda$. The relative wavelength shift $\Delta\lambda/\lambda$ caused by a temperature change ΔT can be expressed as [23];

$$\frac{\Delta\lambda}{\lambda} \approx (\alpha+\xi)\Delta T \quad (5)$$

Table 1 Taper profiles with waist diameters fixed at d = 10 μm, their FSR and sensitivity are also presented.

Sensor ID	*a* (mm)	*b* (mm)	*c* (mm)	*d* (μm)	FSR (nm)	Sensitivity (pm/°C)
S1	4	4	4	10	7.6	45.5
S2	4	8	4	10	6.2	32.1
S3	4	10	4	10	3.7	28.0
S4	4	12	4	10	3.2	14.1

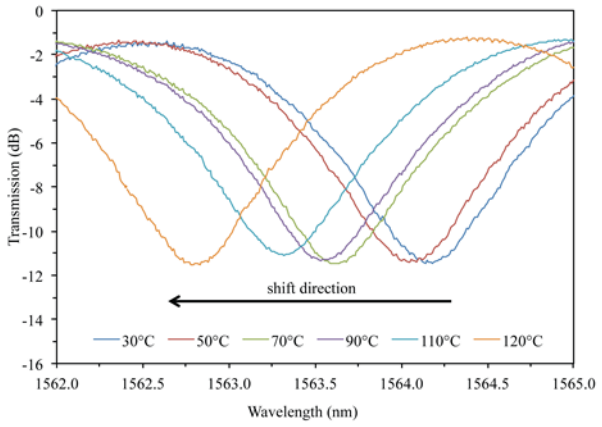

Figure 4 Spectral response of the sensors with variation of tapered fiber profiles. Note that the spectrum shifts are blue-shifted

Figure 4 illustrates the interference spectra of the sensor with tapered waist length and transition lengths of 12 mm and 4 mm, respectively, at different temperatures (30°C, 50°C, 70°C, 90°C, 110°C and 120°C). Note that the interference peaks show a consistent shift towards the shorter wavelength region when temperature was increased. The result obtained is in good agreement with previously reported studies [24], [25]. The blue-shift observation is due to the negative thermo-optic coefficient value for air. The FSR and fringe visibility were measured to ~3.42 nm and ~10 dB around 1565 nm, which are larger than some reported high-temperature sensors [23], [26], thus making the setup suitable for sensing applications.

To further study the temperature responses of the sensor, three taper profiles with different L values, were prepared. Table 1 shows the dimensions of all taper profiles tested in the experiment. Similar blue-

shifted wavelength shift trend was observed in the interference spectra when temperature was increased. The sensor's performance of each taper profile was evaluated by calculating its temperature sensitivity. The temperature sensitivity, *S*, of the sensor is defined as the interference wavelength shift divided by the corresponding temperature change. It is represented by the gradient of the linear curve in the plot of wavelength shift versus temperature. As shown in Figure 5, all plots revealed a negative slope due to the wavelength blue-shift with R^2 value of greater than 90%. It is also observed that S is inversely proportional to the *L*, as it decreases from 45.5 pm/°C to 0.0141 nm/°C for lengths from 12 mm to 4 mm.

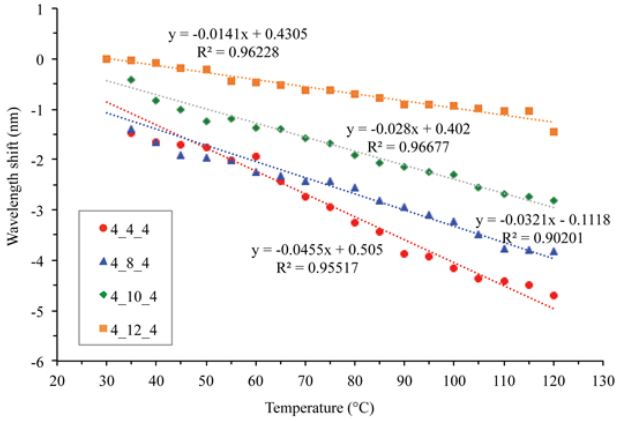

Figure 5 Sensitivity plots of the sensors. All plots show a negative slope as the spectrum shift to a shorter wavelength (blue-shifted)

This observation can be explained by the Eq. (3), where *L* is inversely proportional to FSR, creating smaller wavelength shifts as the *L* increases, hence, the decrease in sensitivity. Therefore, *L* will be the main parameter to be manipulated during the sensitivity optimization of the sensor. Based on our results, taper profile S1 with the smallest waist length exhibited the best sensitivity at 45.5 pm/°C. Ideally, the temperature range that can be measured by the sensor is higher than 120^{0}C as the fused silica fiber material is used to fabricate this sensor, which has high melting point. However, we are unable to test the sensor for a high temperature application due to the limited capability of the oven. The OSA wavelength resolution is 0.01 nm, so the temperature resolution of the sensor is 1^{0}C.

Despite the simple fabrication of our sensor, their performance is comparable with previously reported temperature sensors. In fact, the sensitivity is better than the one reported in [27]. With this clear advantage compared to other fabrication methods that involve more complicated setups, our simple and reproducible fabrication method proves to be a better alternative. However, the sensitivity of the sensor can be further enhanced by depositing temperature-sensitive or thermochromics materials to the taper waist region. Sensor packaging is another important factor for high temperature measurement as it will increase the mechanical strength of the sensor for real applications. Surface modification and packaging will be investigated in our future work on temperature sensors.

4.0 CONCLUSION

In conclusion, we have shown that the waist length of the tapered fiber plays a crucial part in enhancing the sensitivity of the temperature sensors. The sensitivity increases from 0.0141 nm/°C to 0.0455 nm/°C when the waist length was decreased from 12 mm to 4 mm. The optimum profile according to our results was achieved with taper profile S1 that obtained a sensitivity value of 0.0455 nm/°C. Among the highlighted advantages of our sensor are its simple fabrication procedures and high reproducibility compared to the existing sensors based on tapered optical fiber. Despite its simplicity, the temperature sensitivity exhibited by this sensor is comparable with other tapered-fiber based temperature sensors.

Acknowledgement

This work was partly supported by the three years scholarship of Academic Training Scheme for Institutions of Higher Education (SLAI), Ministry of Higher Education (MOHE), Malaysia and the Universiti Putra Malaysia-MHOE Malaysia (research grant #GP-IPB/2014/9440700). We would also like to thank Siti Azlida Ibrahim and Mas Izyani Md Ali for their technical input on this work.

References

[1] Grattan, K. 2000. Fiber Optic Sensor Technology: An Overview. *Sensors and Actuators A: Physical.* 82: 40-61.
[2] Wang, P., Y. Semenova, Q. Wu, and G. Farrell. 2011. A Fiber-optic Voltage Sensor Based on Macrobending Structure. *Opt. Laser Technol.* 43: 922-925.
[3] Guo, H., G. Xiao, N. Mrad, and J. Yao. 2011. Fiber Optic Sensors for Structural Health Monitoring of Air Platforms. *Sensors (Basel).*11(4): 3687-705.
[4] Zhu, T., D. Wu, M. Liu, and D. W. Duan. 2012. In-Line Fiber Optic Interferometric Sensors in Single-Mode Fibers. *Sensors (Switzerland)*. 12(8): 10430-10449.
[5] Li, Y., C. Wen, Y. Sun, Y. Feng, and H. Zhang. 2014. Capillary Encapsulating of Fiber Bragg Grating and the Associated Sensing Model. *Opt. Commun.* 333: 92-98.
[6] Li, Q. S., X. L. Zhang, H. He, Q. Meng, J. Shi, J. N. Wang, and W. F. Dong. 2014. Improved Detecting Sensitivity of Long Period Fiber Gratings by Polyelectrolyte Multilayers: the Effect of Film Structures. *Opt. Commun.* 33: 39-44.
[7] Liu, Y., W. Peng, Y. Liang, X. Zhang, X. Zhou, and L. Pan. 2013. Fiber-optic Mach-Zehnder Interferometric Sensor for High-sensitivity High Temperature Measurement. *Opt. Commun.* 300: 194-198.
[8] Rajan, G., M. Ramakrishnan, Y. Semenova, K. Milenko, P. Lesiak, A. W. Domanski, T. R. Wolinski, and G. Farrell. 2012.

A Photonic Crystal Fiber and Fiber Bragg Grating-Based Hybrid Fiber-Optic Sensor System. *IEEE Sens. J.* 12(1): 39-43.
[9] Lim, K. S., I. Aryanfar, W. Y. Chong, Y. K. Cheong , S. W. Harun and H. Ahmad. 2012. Integrated Microfibre Device for Refractive Index and Temperature Sensing. *Sensors*. 12: 11782-11789.
[10] Mescia, L. and F. Prudenzano. 2013. Advances on Optical Fiber Sensors. *Fibers*. 2(1): 1-23.
[11] Ji, W. B., H. H. Liu, S. C. Tjin, K. K. Chow, and A. Lim. 2012. Ultrahigh Sensitivity Refractive Index Sensor Based on Optical Microfiber. *IEEE Photonics Technol. Lett.* 24(20): 1872-1874.
[12] Zibaii, M. I., H. Latifi, Z. Saeedian, and Z. Chenari. 2014. Nonadiabatic Tapered Optical Fiber Sensor for Measurement of Antimicrobial Activity of Silver Nanoparticles Against Escherichia coli. *J. Photochem. Photobiol. B Biol.*135: 55-64.
[13] Tian, Y., W. Wang, N. Wu, X. Zou, X. Wang, and B. D. Program. 2011. Tapered Optical Fiber Sensor for Label-Free Detection of Biomolecules. *Sensors (Basel, Switzerland)*. 11: 3780-3790.
[14] Lin, H. Y., C. H. Huang, G. L. Cheng, N. K. Chen, and H. C. Chui. 2012. Tapered Optical Fiber Sensor Based on Localized Surface Plasmon Resonance. *Opt. Express.* 20(19): 21693-701.
[15] Lee, C-H., J. Lee, M-K Kim and K-T Kim. 2011. Characteristics of a Fiber Bragg Grating Temperature Sensor Using the Thermal Strain of an External Tube. *Journal of the Korean Physical Society*. 59(5): 3188-3191.
[16] Yun, L., W. Peng, Y. Liang, X. Zhang, X. Zhou and L. Pan. 2013. Fiber-optic Mach–Zehnder Interferometric Sensor for High-Sensitivity High Temperature Measurement. *Optics Communications.* 300: 194-198.
[17] Black, R. J., S. Lacroix, F. Gonthier, and J. D. D. Love. 1991 Tapered Single-Mode Fibres and Devices. Pt. 2: Experimental And Theoretical Quantification. *IEE Proc. J.* 138(5): 355-364.
[18] Harun, S. W., K. S. Lim, C. K. Tio, K. Dimyati, and H. Ahmad. 2013. Theoretical Analysis and Fabrication of Tapered Fiber. *Opt.-Int. J. Light Electron Opt.*124(6): 538-543.
[19] Ravets, S., J. E. Hoffman, P. R. Kordell, J. D. Wong-Campos, S. L. Rolston, and L. A. Orozco. 2013. Intermodal Energy Transfer in a Tapered Optical Fiber: Optimizing Transmission. *J. Opt. Soc. Am. A. Opt. Image Sci. Vis.* 30(11): 2361-71.
[20] Nguyen, L. V., D. Hwang, S. Moon, D. S. Moon, and Y. Chung. 2008. High Temperature Fiber Sensor with High Sensitivity Based on Core Diameter Mismatch. *Opt. Express*. 16(15): 11369-11375.
[21] Okamoto, K. *Fundamental of Optical Waveguides.* 2006. London: Academic Press.
[22] E. M. J. Weber, A. V Dotsenko, L. B. Glebov, and V. A. Tsekhomsky, *Handbook of Optical Materials.* 2003. New York: CRC Press.
[23] Li, E., X. Wang, and C. Zhang. 2006. Fiber-optic Temperature Sensor Based on Interference of Selective Higher-Order Modes. *Appl. Phys. Lett.* 89(9): 091119.
[24] Xu, B., J. Li, Y. Li, J. Xie, and X. Dong. 2014. Liquid Seal for Temperature Sensing with Fiber-Optic Refractometers. *Sensors*. 14(8): 14873-4884.
[25] Yadav, T., M. A. Mustapha, M. H. Abu Bakar and M. A. Mahdi. 2014. Study of Single Mode Tapered Fiber-optic Interferometer of Different Waist Diameters and Its Application As A Temperature Sensor. 14024: 8-12.
[26] Monzón-Hernández, D., V. P. Minkovich, and J. Villatoro. 2006. High-temperature Sensing with Tapers Made of Microstructured Optical Fiber. *IEEE Photonics Technol. Lett.* 18(3): 511-513.
[27] Kieu, K. Q. and M. Mansuripur. 2006. Biconical Fiber Taper Sensors. *IEEE Photonics Technol. Lett.* 18(21): 2239-2241.